INTERNATIONAL JOURNAL OF INNOVATIVE RESEARCH

IN COMPUTER & COMMUNICATION ENGINEERING

INTERNATIONAL STANDARD SERIAL NUMBER INDIA

Impact Factor: 8.379

Design and Simulation of Bow-Tie Antenna for GPR Applications

Sanjai B, Sanjai K[1], Sarvesh M.D[2], Sangeeth V[3], Kavitha A[4]

UG Student, Dept. of ECE., M. Kumarasamy College of Engineering, Karur, Tamil Nadu, India[1 2 3]

Professor, Dept. of ECE, M. Kumarasamy College of Engineering, Karur, Tamil Nadu, India[4]

ABSTRACT: In this paper presents a low-profile bowtie antenna loaded by a rectangular array of artificial magnetic conductor metasurface (AMC) for ground penetrating radar (GPR) applications. The proposed antenna operates from 200 MHz to 400 MHz, with stable radiation characteristics. The proposed work presents several novel aspects, including the unconventional placement of the AMC structure directly at the back of the substrate without any separation to maintain the design simplicity and robustness. This utilization of AMC unit cells results in bandwidth improvement and gain enhancement. An analytical formula for the reflection coefficient has been introduced and compared to full wave simulation to investigate AMC partial reflectivity at low frequencies. The prospective antenna has a size of 6 ×6 cm and covers a vast fractional bandwidth (FBW) of 79.4%, which is significantly higher than the conventional bowtie antenna's 20% FBW. Furthermore, a back reflector is placed at 33.3 cm from the antenna to eliminate the back radiation, avoid unwanted clutters during the GPR measurements and increase the antenna gain using an AMC Surface.

KEYWORDS: Bow-Tie antenna, equivalent circuit, GPR, metamaterial.

I. INTRODUCTION

Ground-penetrating radar (GPR) is a well-known non-destructive geophysical technique. It can be used to identify natural geologic materials. Currently, GPR is employed to detect other media such as wood, concrete, and asphalt. GPR can be also used for road quality assessment, buried objects detection, and civil engineering [1], [2]. GPR systems can be classified into two categories: a continuous wave that works in the frequency domain, and impulse wave, which works in the time domain. Impulse-based GPR systems are less complex and cost-effective [2]. Antenna stage is one of the most critical parts of the GPR system. Basically, antenna performance characteristics required for the GPR applications, i.e., linear polarization, ease of design and fabrication, better symmetry in radiation pattern. Till now, many antenna types have been reported for GPR applications. Two main types of antennas have the greatest interest in the GPR research field [3]. The first category is the air-coupled antennas which are normally 40-50 cm above the ground surface, such as horn antennas and tapered slot antennas (TSA) [4], [5]. This category suffers from the bulky size as well as the strong mutual coupling between the transmitter and receiver. The second category is the ground-coupled antennas of planar structure, such as loaded dipole [6], spiral [7], microstrip monopole [8], bowtie antenna and, its variants [9]. The ground-coupled antennas are appropriate for working close to the ground surface; 5-10 cm above the ground. Bowtie antenna is the most popular structure for commercial GPR devices due to its excellent radiation performance [10]–[12]. The influence of the geometrical configuration and input impedance of bowtie antennas on the reflected signal strength from a near-surface object is investigated [10]. Although the bowtie antennas successfully applied for the GPR systems. However, low gain, narrow bandwidth especially at low frequencies, and high dispersion of frequency spectrum cause several limitations.

Furthermore, several techniques have been reported to improve the conventional bow-tie antennas performance. Ref. [13] review some of these modifications such as the structural modification technique, which is effective solely in the high frequency range but can't be applied in lower frequencies. Resistive loading is used for reducing the lower cut-off frequency and also reducing the antenna ringing, i.e., multiple reflections between the feed point and the open end of the bow-tie antenna due to the abrupt impedance change in the impedance level at either side of the antenna [14]. However, resistive loading is degrading the antenna radiation efficiency significantly. Reduction in radiation efficiency can be significantly minimized by using capacitive loading with resistive loading. Array configuration was proposed to improve the radiation efficiency and front to back ration (F/B) [15], also it can be enhanced using a cavity [16], [17].

Recently, metamaterials have been used for the same purpose [18]. However, the radiation properties improve at the cost of size and complexity of the bow-tie antennas. A paddle shaped microstrip antenna was proposed as a modified version of the Bowtie antenna by cutting a rectangular patch at one of its diametrical edges fed by the coplanar waveguide technique. The antenna is loaded by stubs, shorting pins, and a split-ring resonator (SRR) metamaterial structure to increase the antenna gain and enhance the bandwidth (BW) towards both the lower and higher end of the working BW [19]. A grooved elliptical patch with a corrugated semi-elliptical ground plane was developed to improve the antenna bandwidth [20]. Bowtie cage antenna consists of two thick diverging cages composed of 10 cylindrical metallic rods was developed to improve the antenna bandwidth [21]

Although all the previous literature has been contributed to bandwidth and gain improvement, all work suffers from either complexity or the low frequency operating bandwidth. In this paper, a modified structure of bow-tie antenna is introduced for low frequency GPR applications. The prospective antenna is operating at the bandwidth ranging from 1.168 GHz to 1.357 GHz. This work is innovative due to the AMC matrix metasurface's design being placed directly on the backside of the antenna, without any separation as seen in traditional designs, which eliminates the surface wave and enhances both the antenna gain and directivity. A metallic reflector is further added behind the AMC metasurface to improve the antenna gain at the lower frequencies. A transmission line model is introduced to study the reflectivity of the metasurface structure. The simulation model is analyzed using High Frequency Structure Simulator (HFSS). To the best of our knowledge, no work has been reported for the low frequency GPR antenna, with AMC attached directly to the antenna to improve the gain, the bandwidth and maintain the antenna robustness.

II. ANTENNA DESIGN

A. *AMC Meta surface Reflectivity:*
In this section, a square periodic patch is chosen because it has a large in-phase band compared to other AMC structures which have a compact size at the expense of bandwidth [22]. Fig.1 (a) shows the configuration of the suggested square AMC unit cells including the dimensions parameters. Fig.1 (b) shows the HFSS simulation setup for AMC. The AMC rectangular unit cell is excited through horizontal plane wave with electric field direction perpendicular to the PEC walls.

To study the reflectivity of the rectangular periodic AMC unit cells at different frequencies, equivalent circuit model is employed as shown in Fig.1(c) Consequently, the reflection coefficient can be given by

$$\Gamma = \frac{Z_{in} - \eta_{eff}}{Z_{in} + \eta_{eff}} \qquad (1)$$

Where η_{eff} is the effective wave impedance inside dielectric material

Z_{in} the input impedance referring to boundary surface at dielectric slab and air.

$$Z_{in} = \eta_{eff} \frac{Z_{load} + j\eta_{eff} \tan(k_{eff}h)}{\eta_{eff} + jZ_{load} \tan(k_{eff}h)} \qquad (2)$$

k_{eff} is the wave number in the dielectric material

Z_{load} is parallel connection for grid impedance and the air wave impedance which is represented by:

$$Z_{load} = \frac{Z_g \eta_o}{Z_g + \eta_o} \qquad (3)$$

Z_g is the grid impedance which is related to the tangential electric field in the meta surface plane and the induced surface current density on it.

$$Z_g^{TM,TE} = -j\frac{\eta_{eff}}{2\alpha} \qquad (4)$$

α is grid parameter [23] and it has the following form:

$$\alpha = \frac{2\,fa\sqrt{\varepsilon_{eff}}}{c}\ln(\csc(\frac{\pi s}{2a})) \qquad (5)$$

Based on the abovementioned analytical formulations, the reflection at air-dielectric boundary for a normal incident plane wave is calculated using MATLAB software. For verification, a full wave simulator HFSS is utilized for the same purpose.
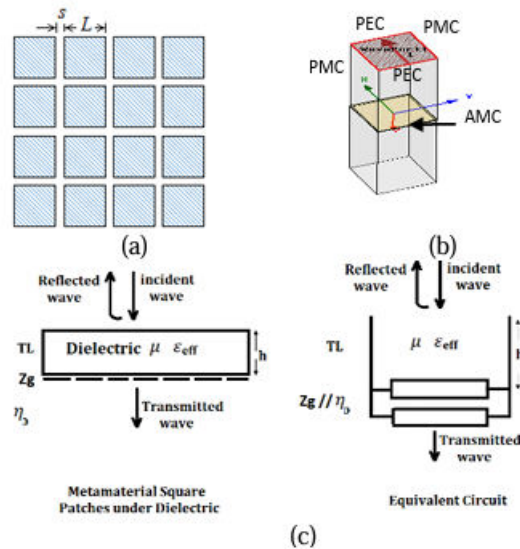

Fig.1. (a) Configuration of square AMC (L=9cm, s=0.5cm) (b) HFSS Simulation setup for AMC (c) The transmission line model for square patch grid on one side of dielectric slab.

B. *Design Methodology:*

In this section, the conventional bowtie antenna is presented as an initial design to our proposed modified structure and the operating center frequency is selected at 1.25GHz. Bowtie shape is a conventional design for a GPR antenna, cutting the edges of the bowtie help to reduce the antenna's overall size while also affecting its characteristic impedance. Chen et al. [24] discuss 3 different shapes for edge cutting and recommend the shape at which the length of straight part of one arm equal 0.25 of the total antenna length. The length of the bowtie L is directly related to half of the lower frequency's wavelength, while the flare angle affects the bandwidth, a larger flare angle leads to a wider bandwidth. The optimal range for flare angle is typically between 60 and 90 degrees to achieve both a wideband performance and a compact design. The bowtie's length is initially determined by formula:

$$L = \frac{\lambda}{2\sqrt{\varepsilon_{reff}}} \qquad (6)$$

Where, λ is wavelength at lower operating frequency. however, simulation is used to refine the lengths to achieve accurate resonance at 0.2 GHz. Fig.3 shows the geometry for the initial design; W=14.4 cm, L=2.64 cm, and L1=2.93 cm. The antenna is mounted on FR4 substrate with relative permittivity 4.4 and a thickness 1.6 mm. A narrow bandwidth of about 40MHz and a 2.13 dBi gain are attained.
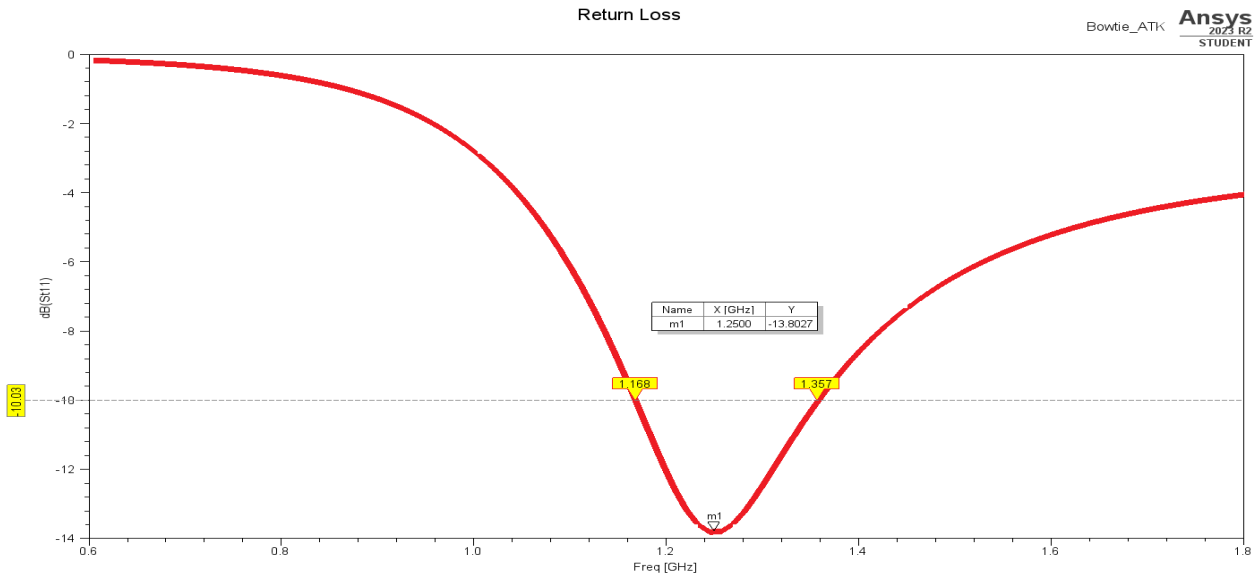
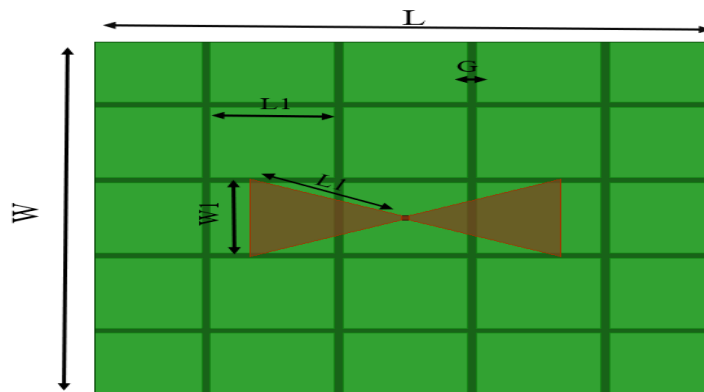Fig.2. Return loss and geometry for simple Bow-Tie antenna

Fig.3. Proposed Bow-Tie antenna.

To improve the antenna bandwidth, a 5×5 square AMC metasurface unit are arranged on the antenna backside with 0.16cm periodic gaps. Placing the planar AMC metasurface close to antenna structure as shown in Fig. 4 influences the antenna surface current distribution thus antenna characteristic; gain, and impedance matching are affected.

Table 1: Antenna and AMC dimensions

Parameter	Value [cm]
L	12
W	12
W1	2.64
L1	2.93
L2	2.4
G	0.16

To enhance the gain in the low frequencies where meta-surface is partially reflective, a full metallic reflector is positioned back to the AMC plan. The distance between the antenna and the metallic reflector is optimized to introduce a constructive interference for reflected waves and the radiated one from Bow-Tie antenna.

C. *Equivalent Circuit Model for Antenna Loaded by AMC*

In this section, we establish a lumped model as depicted in Fig.6 by utilizing the resonant frequency of the bowtie antenna and the AMC structure. This model comprises a set of RLC resonant circuits that represent the radiating element, and a capacitor and inductor parallel to the gap capacitor to represent the periodic structure of the AMC. The complete equivalent circuit is obtained by linking the RLC bowtie antenna model to the AMC model. To analyze the performance of the bowtie antenna augmented by AMC, we used ADS circuit simulator software to simulate the equivalent circuit. Fig.7 demonstrates that the results of the ADS and HFSS reflection coefficient that show very good agreement. Notably, the bandwidth of the antenna is heavily influenced by the AMC. The optimum values of RLC circuit are listed in table 2.
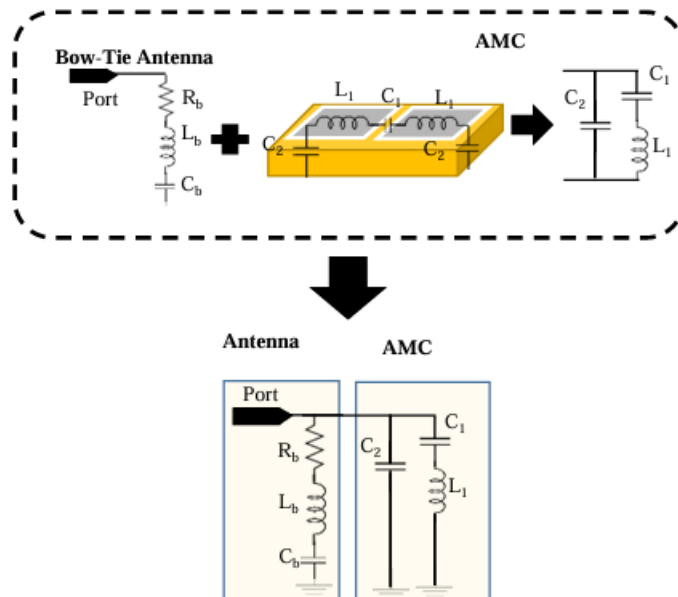

Fig.4. Equivalent circuit of loaded antenna.

Table 2: Equivalent circuit lumped elements values

R_b (Ω)	L_b(nH)	$C_b(pF)$
38.062	22.0078	21.0079
$C_1(pF)$	$C_2(pF)$	L_1(nH)
32.0068	11.0089	62.0038

III. SIMULATION AND MEASUREMENT RESULTS

To validate the simulation results, the proposed bowtie antenna over the AMC structure is fabricated and practically measured, as shown in Figure 4. Both measured and simulated results of reflection coefficient are depicted in Figure 3, which demonstrate that, on the basis of the low profile, the antenna operates at 1.168GHz to 1.357Ghz, with a wide relative impedance bandwidth of 42.04%, while the simulated relative impedance bandwidth is 35.6%, covering from 1.68GHz to 1.37 GHz. The discrepancies are caused by the effect of the SMA connector and the fabrication and measurement errors.

Furthermore, the gain of the proposed antenna is also measured and the results are depicted in Figure 10. It illustrates that the antenna achieves a stable gain higher than 2.13 dBi. The measured maximum gain is up to 2.41 dBi. It can also be noted that the measured gain is slightly lower than the simulated one, which arises from the fabrication and measurement error and the instability of the dielectric substrate.

The radiation patterns of the proposed antenna were measured in an anechoic chamber. The measured radiation patterns at 2.5, 3, and 3.5 GHz are compared with the simulated ones for both E and H planes, as shown in Figure 11. It can be observed from the radiation patterns that the measured and simulated results at the three operating frequencies show good consistency with each other
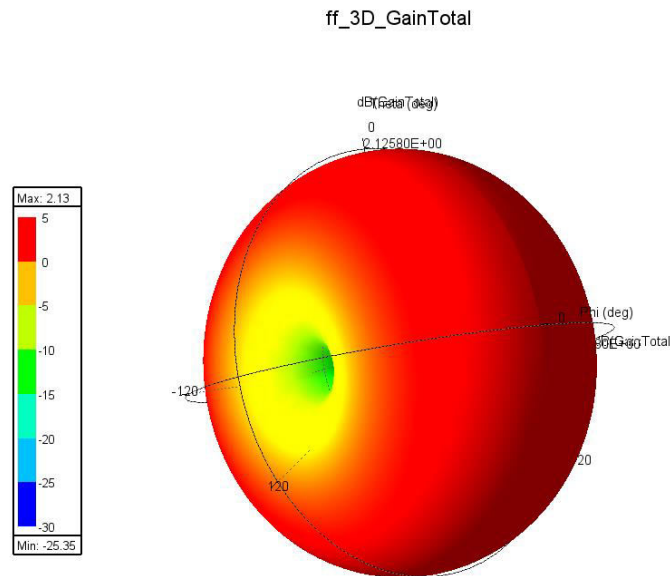

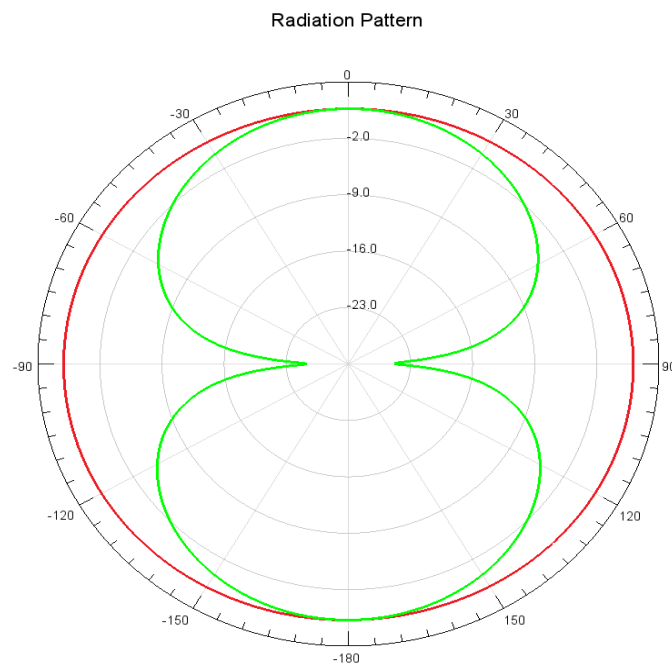
Fig.5 shows 3D Polar Plot for Gain (dB)

Fig.6 shows Radiation Pattern of the Proposed antenna

except for some shaking in the measured cross-polarization and the back lobes of the measured co-polarizations, probably caused by the noises in the anechoic chamber. The measured front-to-back ratios are less than -14 dB at the three frequencies. The measured maximum cross-polarization level is -17 dB for both E and H planes. Compared with previously designed AMC-based bowtie antennas (see Table 3), the proposed antenna achieves broad band and high gain with maintaining low profile.

Table 3: Comparison with other GPR antennas

Reference	Antenna type	Structure	Size in cm	Largest dimension w.r.t largest wavelength in air	Approx. avg. gain in dBi	BW in GHz (gain> 0dBi, S11<-8 dB
[4]	Flare horn	3D	25.6 × 19 × 8.6	0.5λ	_ _ _	0.6-6
[25]	Slot	flat	10.67 × 6.8	0.5λ	4.7	1.4-3.5
[26]	Tapered slot	flat	18 × 22	0.44λ	4	0.6-4
[27]	Folded bowtie	3D	18x28.2x15	0.5λ	4	0.55-0.85
[28]	Monopole	3D	20.8 ×16.9 ×19.05	0.28λ	4	0.4-3
Proposed work	Bow Tie	flat	12 ×12x0.16	0.3λ	5	0.163-0.357

IV. CONCLUSION AND FUTURE WORK

In this paper, an AMC-based broadband bowtie antenna is proposed for GPR` application. Loaded with two parallel open stubs in the upper layer, the proposed bowtie antenna has the merit of broad band. An AMC surface composed of 5x5unit cells is designed and located under the bowtie antenna with a distance of only one-tenth the free space wavelength at 3.0 GHz for gain enhancement and low profile. Experimental results show that, with maintaining the low profile, the composite antenna achieves a wide bandwidth (return loss -10 dB) of 35.6%, operating from 1.163 to 1.357 GHz. A flat gain from 2.13 dBi are found over the whole band. Measured results demonstrate that the antenna achieves a wide relative frequency bandwidth of 42.04%, operating from 1.163.48 to 1.357 GHz. The measured maximum gain is up to 2.13 dBi. Moreover, low front-to-back ratios and cross-polarization level is obtained simultaneously. Good agreement lies between the measured and simulated results.

REFERENCES

1. P. Taylor, L. Pajewski, and A. Benedetto, "Preface." Nondestruct. Testing and Eval., Vol.27, No. 3 pp. 187 88, Sept. 2012. doi: 10.1080 /10589759. 2012. 710389
2. Huston and D. Busuioc, "Radar technology: radio frequency, interferometric, millimeter wave and terahertz sensors for assessing and monitoring civil infrastructures," in Sensor Technol. for Civil Infrastructures, Vol.55, pp. 201–237, May 2014. doi: 10.1533/9780857099136.201.
3. N. Diamanti and A. P. Annan, "Air-launched and ground-coupled GPR data," in 2017 Eur. Con. on Antennas and Propa.(EUCAP), Paris, France, pp. 1694–98, Mar. EuCAP.2017.7928409.
4. Ahmed, Y. Zhang, D. Burns, D. Huston, and T. Xia, "Design of UWB antenna for air-coupled impulse ground-penetrating radar," IEEE Geosci. and Remote Sens. Lett., Vol.13, No. 1, pp. 92–96, Jan. 2016. doi:10.1109/LGRS.2015.2498404.
5. B. Wu, "Design and measurement of compact tapered slot antenna for UWB microwave imaging radar," IEEE Int. Conf. on Electron. Meas. & Instrum., Beijing, China: IEEE, pp. 2-226-2–22. & Instrum., Beijing, China: IEEE, pp. 2-226-2–229, Aug. 2009. Doi:10.1109/ICEMI.2009.5274613.
6. Lee, "Investigation of the pulse radiating performance of resistively loaded dipole antennas by manipulation of the loading parameter," AEU – Int. J. of Electron. and Commun., Vol. 98, pp. 248–58, Jan. 2019, doi: 10.1016/j.aeue.2018.11.003.

7. N. Liu, P. Yang, and W. Wang, "Design of a miniaturized ultra-wideband compound spiral antenna," IEEE Int. Conf. on Microw. Technol. & Comput. Electromagn., Qingdao, China, pp.255–58, Aug. 2013. doi: 0.1109/ICMTCE.2013.6812453.

8. Raza, W. Lin, Y. Liu, A. B. Sharif, Y. Chen, and C. Ma, "A magnetic-loop based monopole antenna for GPR applications," Microw. Opt. Technol. Lett., Vol. 61, No. 4, pp. 1052–1057, Apr. 2019, doi: 10.1002/mop.31690.

9. Mr. Rajesh N. I. Medhat, A. S. A. El-hameed, and M. Sato, "Application of cross -Bowtie antenna to detection of buried pipes by GPR" IEICE Tech. Rep., Vol. 119, No.121, pp.61-66, July 2019.

10. X. Gao, F. J. W. Podd, W. Van Verre, D. J. Daniels, and A. J. Peyton, "Investigating the performance of Bi-static GPR antennas for near-surface object detection," Sensors, Vol. 19, No. 1, p. 170, Jan. 2019, doi: 10.3390/s19010170.

11. J. Ali, N. Abdullah, M. Yusof, E. Mohd, and S. Mohd, 7, "Ultra-Wideband antenna design for GPR applications: a review," Int. J. of Adv. Comput. Sci. and App., Vol. 8, No. pp. 392–400, doi: 10.14569/ijacsa.2017.080753.

12. Warren and A. Giannopoulos, "Creating finite difference time-domain models of commercial ground- penetrating radar antennas using Taguchi's optimization method," Geophysics, Vol. 76, No. 2, pp. G37–G47, Mar. 2011, doi: 10.1190/1.3548506.

13. R. Nayak, S. Maiti, R. Nayak, and S. Maiti, "A review of Bow-tie antennas for GPR applications," IETE Technical Review, Vol. 36, No.4, pp. 382–397, Jul. 2019, doi: 10.1080/02564602.2018.1492357.

14. Raza, W. Lin, M. K. Ishfaq, M. Inam, F. Masud, and M. H. Dahri, "A Wideband reflector-backed antenna for applications in GPR," Int. J. Of Antennas and Propag., ,Nov. 2021.

15. Y. Ren and C. Lai, "Wideband antennas for modern radar systems," Radar Technology. InTech, Jan. 2010. doi: 10.5772/7187.

16. S. Liu, M. Li, H. Li, L. Yang, and X. Shi, "Cavity backed bow-tie antenna with dielectric loading for ground-penetrating radar application," IET Microw. Antenna Propag., Vol.14, No.2, pp. 153–157, Feb. 2020, doi: 10.1049/ iet-map.2019.0309.

17. Elsherbini, J. Wu, and K. Sarabandi, "Dual polarized wideband directional coupled sectorial loop antennas for radar and mobile base-station applications," IEEE Trans. Antennas Propag., Vol. 63, No. 4, pp. 1505 1513, Apr. 2015, doi: 10.1109/TAP.2015.2392773.

18. K. K. Ajith and A. Bhattacharya, "printed compact lens antenna for UHF band applications," Prog. In Electromagn. Research C, Vol. 62, pp. 11–22, Jan. 2016, doi: 10.2528/PIERC15112702.

19. T. Saeidi, A. R. H. Alhawari, A. H. M. Almawgani, T. Alsuwian, M. A. Imran, and Q. Abbasi, "High gain compact UWB antenna for ground penetrating radar detection and soil inspection," Sensors, Vol. 22, no 14, p. 5183, Jul. 2022. doi: 10.3390/s22145183.

20. M. Guerrouj, A. Chaabane, and A. Boualleg, "Super UWB grooved and corrugated antenna for GPR application super UWB grooved and corrugated antenna for GPR application," Period. Polytech. Elec. Eng. Comp. Sci., Vol. 66, No. 1, pp. 31–37, Jan. 2022, doi: 10.3311/PPee.17221.

21. G. Kumar, M. B. Mahajan, P. Mevada, and S. Chakrabarty, "Ultrawide band cage dipole antenna for ultra-high frequency band ground penetrating radar system," Int J RF Microw. Comp-Aid Eng, Vol. 32, No. 6, p. e23139, Jun. 2022, doi: 10.1002/mmce.23139.

22. R. Dewan et al., "Artificial magnetic conductor for various antenna applications: An overview," Int J RF Microw. Comp-Aid Eng, Vol. 27, No. 6, pp. 1–18, Aug. 2017, doi: 10.1002/mmce.21105.

23. O. Luukkonen, C. Simovski, G. Granet, and G. Goussetis, "Simple and accurate analytical model of planar grids and high-impedance surfaces comprising metal strips or patches," IEEE Trans. Antennas Propag., Vol. 56, No. 6, pp. 1624–1632, Jun. 2008, doi: 10.1109/TAP.2008.923327.

24. Guo Chen and R. C. Liu, "A 900MHz shielded bow-tie antenna system for ground penetrating radar," Proc. of the XIII Int. Conf. on Ground Penetrating Radar, pp.1 6, Jun. 2010, doi: 10.1109/icgpr.2010.5550125.

25. M. Li, R. Birken, N. X. Sun, and M. L. Wang, "Compact slot antenna with low dispersion for ground penetrating radar application," IEEE Antennas and Wireless Propag. Lett., Vol. 15, pp. 638–641, Aug. 2015, doi: 10.1109/lawp.2015.2465854.

26. Raza, W. Lin, Y. Chen, Z. Yanting, H. T. Chattha, and A. B. Sharif, "Wideband tapered slot antenna for applications in ground penetrating radar," Microw. and Optical Techn. Lett., Vol. 62, No. 7, pp. 2562–2568, Mar. 2020, doi: 10.1002/mop.32338.

27. G. Yang, S. Ye, Y. Ji, X. Zhang, and G. Fang, "Radiation Enhancement of an Ultrawideband unidirectional folded Bowtie antenna for GPR applications," IEEE Access, Vol. 8, pp. 182218 182228, Oct. 2020, doi: 10.1109/access.2020.3029050.

28. P. Srimuk, A. Boonpoonga, K. Kaemarungsi, K. Athikulwongse, and S. Dentri, "Implementation of and experimentation with ground-penetrating radar for real time automatic detection of buried improvised explosive devices," Sensors, Vol. 22, No. 22, p. 8710, Nov. 2022, doi: 10.3390/s22228710.

INTERNATIONAL JOURNAL OF INNOVATIVE RESEARCH

IN COMPUTER & COMMUNICATION ENGINEERING

9940 572 462   6381 907 438   ijircce@gmail.com

Scan to save the contact details